# Landfill gas flow – effects of asymmetry

Seth Keenan[a], Yana Nec[b] and Greg Huculak[c]

[a] Department of Chemistry, Thompson Rivers University, Kamloops, British Columbia, Canada
[b] Department of Mathematics and Statistics, Thompson Rivers University, Kamloops, British Columbia, Canada
*e-mail:* cranberryana@gmail.com
[c] GNH Consulting Ltd., Delta, British Columbia, Canada

**Abstract**

Waste disposal is the responsibility of cities throughout the world. The most common method in North America is to bury waste in landfills. Landfill operators comply with regulations to control hazardous emissions known as landfill gas (LFG). The gas is extracted via horizontal or vertical wells and removed from the site. This study examines arrays of horizontal wells placed side by side or stacked, and resultant landfill gas flux between adjacent cells. A landfill's lifetime often sees changes in the number, relative location and efficacy of wells. The ability to predict the response of an array of wells to variation in a single well's functionality is an essential aspect of landfill design and operation. The integrated normal flux between cells is identified as a salient quantity required to construct such prediction models. Numerical solution of flow equations reveals a stunningly simple dependence of the flux on the relative suction strength of proximate cells in a wide range of operational conditions. The flux is one of scarcely few parameters accessible in the field with relative ease and certainty, and thus traceable over time. This property makes the proposed models easy to construct, implement and adjust in practice in custom configurations.

**Keywords**: landfill gas, porous media, asymmetry, multiple horizontal wells, non-negligible gravity effect, flux

# 1 Introduction

The sanitary landfill industry is well supported by theoretical research in such areas as modelling of gas generation (Gioannis et al., 2009; Durmusoglu et al., 2005) and efficiency of collection (Spokas et al., 2006; Barlaz et al., 2009), landfill gas escape (Abichou et al., 2009; Gebert and Groengroeft, 2006), leachate treatment (Wiszniowski et al., 2006), leachate contamination of groundwater (Christensen et al., 2001) and propagation of specific contaminants (Lyngkilde and Christensen, 1992; Barnes et al., 2004). However there are surprisingly few studies that solve the gas flow equations. The older studies obtain solutions in simplified geometries, usually adopting a symmetry assumption (Lu and Kunz, 1981; Wise and Townsend, 2011) or other simplifications (Findikakis and Leckie, 1979; Young, 1989) to render the equations soluble. By contrast the recent studies employ an extensive number of degrees of freedom that enable good data fitting, but obscure the qualitative impact thereof (Feng et al., 2017, 2015).

Adequate spacing of wells is a mainstay decision in the construction of new landfills and expansion of existing ones. In the case of horizontal wells – the common collection means in medium and large landfills – this implies both vertical and lateral distances, effectively partitioning the waste volume into cells and defining their dimensions. Currently landfill design engineers have no access to practicable quantitative models enabling these decisions. Albeit analytical and pseudo-analytical flow solutions exist, evaluation of special functions (Feng et al., 2017; Nec and Huculak, 2019), summation of infinite series (Feng et al., 2015; Nec and Huculak, 2019) or inversion of large matrices (Feng et al., 2015) are involved. Numerical investigations require expensive proprietary software packages, e.g. FlexPDE (Halvorsen et al., 2018) or COMSOL (Feng et al., 2015), as well as experience based estimates of numerous parameters such as depth dependent generation rate, temperature and permeability, possibly with anisotropy (Feng et al., 2015). None of the above is easily performed or obtained in practice. Moreover, even when in possession of such computational tools, the flow field itself is only the first step. To estimate the radius of influence and infer the well spacing, one must experiment with cut-off thresholds that might vary with landfill permeability, dimensions and imposed suction strength (Nec and Huculak, 2019). Bearing in mind that the landfill comprises an array of cells, comprehensive scans of all parameter combinations are tedious and often unenlightening, and the results are sensitive to parameters such as permeability that in reality cannot be estimated accurately.

The landfill gas flow research is fundamentally impeded by the fact that field measurements taken at a given point in time inevitably become irrelevant in only a few months as the waste undergoes degradation, preventing any developed model from serving a meaningful lifetime as a control tool. The system is too complicated to devise time dependent models, whose prediction ability will be moot for the selfsame reason. Furthermore, all studies targeting realistic configurations entail one inherent consequence: the results apply solely to the configuration investigated.

The current study suggests an approach that extracts qualitative features of the flow field in asymmetrically functioning cells based on full numerical simulations, and analyses these so as to allow a juxtaposition with readily available records of production for each well. Thus field operators will be able to calibrate and adjust the models in the course of a landfill's lifetime. Mathematically this implies the existence of self-similar and invariant quantities. Self-similarity is an intriguing type of dependence, where a well chosen scaling or relationship between arguments of a multivariate function effectively reduces the number of arguments. This is a classical method widely used in physics and mathematics, from viscous boundary layers to turbulence and fractals. Herein it is shown that the complex flow field in an array of landfill cells harbours certain self-similar relationships that can be put to practical use in the field without access to sophisticated simulation software. The simplicity of the discovered laws enables predictions for landfills differing in dimensions, waste content and any other construction parameters. The foremost advantage thereof is that the model is built by the landfill operators based on routinely collected data and thus is custom fit to the system in question. The operators are the best acquainted therewith and thus well poised to judge which data are germane in the model construction and how often it must be updated as more data become available.

The analysis begins with a basic unit of two cells, positioned side by side or stacked vertically. The total (integrated) normal flux across the centre line equals the difference in production of the two wells, and thus is a quantity easily accessible in the field. This study charts the dependence of the flux on the relative suction strength of the two wells under general operating conditions and then extends the results to arrays of more than two cells. The models can be constructed in practice via collection of volumetric or mass flow data, and adjusted during the landfill's lifetime.

## 2 Geometry and boundary conditions

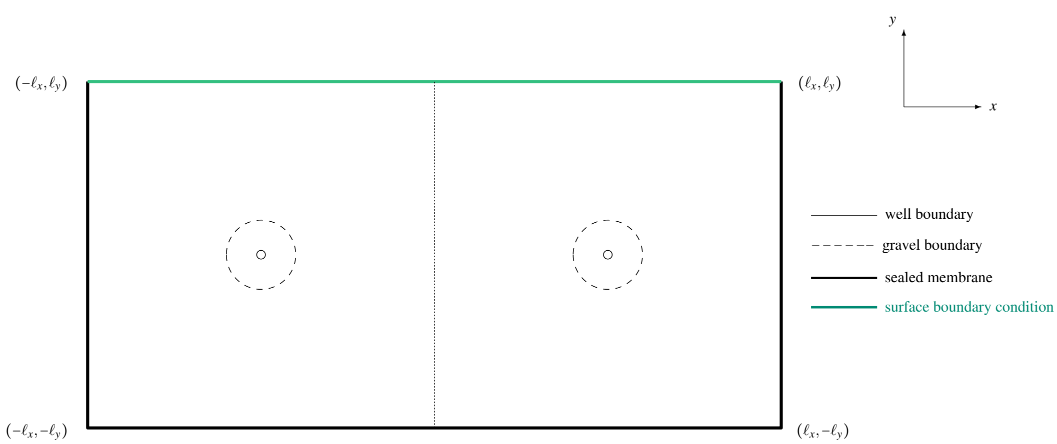


Figure 1: Solution domain for the horizontal $1 \times 2$ configuration (dimensions not to scale)

Consider a landfill comprising two adjacent cells. The configurations depicted in figures 1 and 2 are respectively referred to as horizontal $1 \times 2$ and vertical $2 \times 1$ hereunder. The vertical dimension $\ell_y$ is fixed, whilst the horizontal extent $\ell_x$ is allowed to vary. Aspect ratios in the range $1 \leqslant \ell_x \big/ \ell_y \leqslant 3$ were tested. The landfill bottom and side walls are impermeable, i.e. there is no flow normal to the boundary. On the surface two types of boundary conditions were studied: zero normal flux as above and a fixed pressure value. The latter can be atmospheric or slightly sub-atmospheric, a contingency expected when a cover of fine particle soil is present. In this layer of an extremely low permeability with no gas generation the flow velocity is virtually zero and the fluid pressure distribution is close to hydrostatic (Nec and Huculak, 2019). On the pipe boundaries the pressure equals the respective induced suction values.

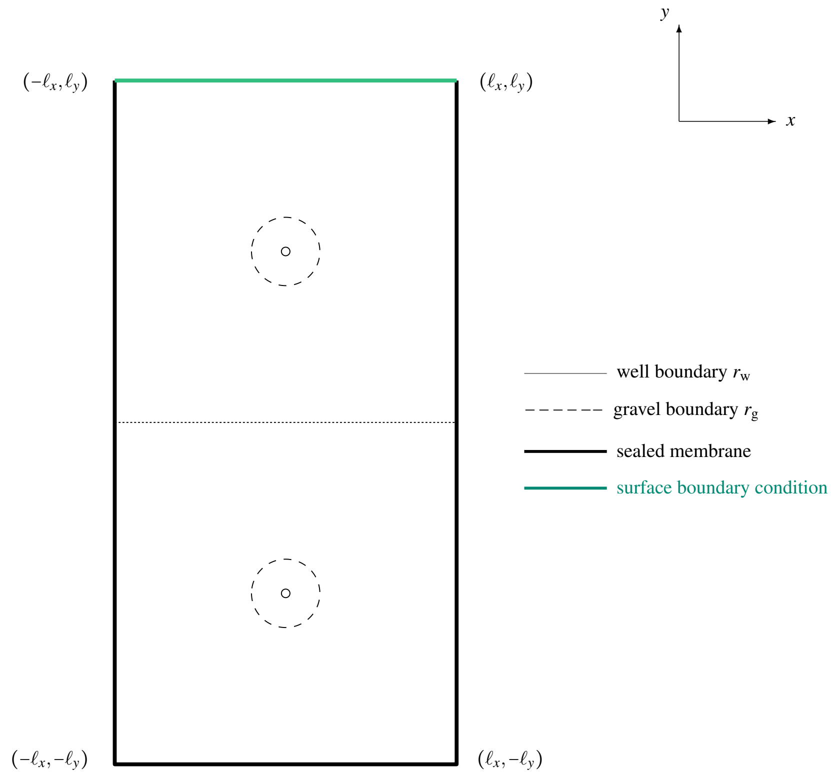


Figure 2: Solution domain for the vertical $2 \times 1$ configuration (dimensions not to scale)

In the horizontal $1 \times 2$ configuration the right well is assigned a nominal pressure value $p_{\mathrm{w_r}}$, here taken in the range $-3.75 \leqslant p_{\mathrm{w_r}} \leqslant -1.25$kPa. The left well can have any value between $p_{\mathrm{w_r}}$ (fully functional) and $p_{\mathrm{atm}}$ (dysfunctional):

$$p_{\mathrm{w_l}} = p_{\mathrm{w_r}} + \Big(p_{\mathrm{atm}} - p_{\mathrm{w_r}}\Big) f_p, \qquad 0 \leqslant f_p \leqslant 1, \tag{1a}$$

wherein $f_p$ determines the relative suction strength between the two wells, and is referred to as the dominance fraction hereinafter. When $f_p = 0$, the suction is equal at both wells. When $f_p > 0$, the right pipe dominates, collecting more gas than the left. With $f_p = 1$ the left pipe is entirely dysfunctional. Due to symmetry there is no need to consider the reverse situation.

The vertical configuration is asymmetric for the fixed surface pressure condition without gravity and for both surface conditions when gravity is accounted for. Hence $f_p$ might be positive (top pipe dominant $p_{\mathrm{w_t}} < p_{\mathrm{w_b}}$) or negative (bottom pipe dominant $p_{\mathrm{w_b}} < p_{\mathrm{w_t}}$):

$$p_{\mathrm{w_b}} = p_{\mathrm{w_t}} + \Big(p_{\mathrm{atm}} - p_{\mathrm{w_t}}\Big) f_p, \qquad 0 \leqslant f_p \leqslant 1, \tag{1b}$$

$$p_{\mathrm{w_t}} = p_{\mathrm{w_b}} - \Big(p_{\mathrm{atm}} - p_{\mathrm{w_b}}\Big) f_p, \qquad -1 \leqslant f_p \leqslant 0. \tag{1c}$$

On the contiguity circle between the gravel and waste layers continuity of pressure and velocity is imposed.

## 3 Equations

For a steady state fluid flow through a porous medium the evolution of momentum is governed by Darcy's law (Whitaker, 1986):

$$\mathbf{u} = -\frac{k}{\mu}\Big(\nabla p - \rho \mathbf{g}\Big), \tag{2a}$$

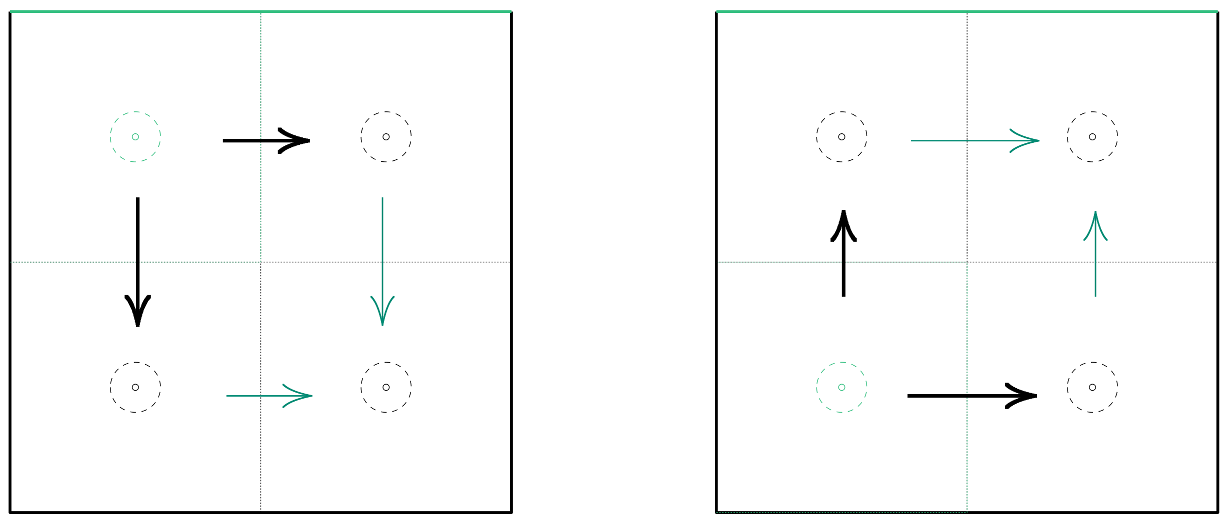

Figure 3: Main (thick black arrows) and residual (thin green/grey arrows) flux diagram for the $2 \times 2$ configuration (dimensions not to scale). The dysfunctional well appears in green/grey. The length of the arrow is commensurate with the flux magnitude. See figure 2 for boundaries legend

where $\mathbf{u}$ is the velocity vector, $k$ – effective permeability value, distinct for each landfill layer, and computable via porosity $\phi$, tortuosity $\tau$ and average waste fragment size (Panda and Lake, 1994). $\nabla p$ denotes pressure gradient (non-constant). Viscosity of the gas $\mu$ was computed based on molar fractions as described in Davidson (1993). $\rho$ is the fluid density and $\mathbf{g} = (0, -g, 0)^{\mathrm{T}}$ the gravity vector. The mass conservation equation in a porous medium reads (Fulks et al., 1971)

$$\frac{\partial}{\partial t}(\phi\rho) + \nabla \cdot (\rho \mathbf{u}) = C, \tag{2b}$$

with the generation rate $C$ non-zero in the waste layer only. The value of porosity in (2b) is immaterial for the purpose of a steady state solution. To form a closed system of equations, the equation of state for the gas is required. The thermodynamic conditions in the landfill justify the assumption of an ideal gas, and hence

$$p = \frac{\rho}{RT}, \tag{2c}$$

with $R$ denoting the gas constant of the mix and $T$ – the effective temperature (Young, 1989). The variation along the well is slow, allowing for an approximation of a two-dimensional flow field within each cross-section (Nec and Huculak, 2019). Thus system (2) is to be solved in planar domains as in figures 1 and 2. The velocity vector $\mathbf{u}$ can then be written as $\mathbf{u} = (u, v)$, where $u$ and $v$ are the horizontal and vertical components respectively. The foremost focus of this study is the qualitative modelling of integrated quantities that bear on observations in the field. One such quantity is the flux across the centre line of the domain induced by asymmetry, be it due to gravity or unequal suction application. In the horizontal $1 \times 2$ configuration the flux is defined as

$$F_{1\times 2} = \int_{-\ell_y}^{\ell_y} \rho u \, \mathrm{d}y, \tag{3a}$$

and similarly for the vertical one

$$F_{2\times 1} = \int_{-\ell_x}^{\ell_x} \rho v \, \mathrm{d}x. \tag{3b}$$

These basic configurations serve as a fundamental unit in the analysis of more complicated arrays of landfill cells: $1 \times 3$, $3 \times 1$ and $2 \times 2$. The purpose is to show that under a variety of conditions a problem of a larger array can be simplified, so that the results for a relevant pair of cells become immediately applicable. The conditions on the rectangular boundary of the $1 \times 3$, $3 \times 1$ and $2 \times 2$ configurations remain the same as in figures 1 and 2. In the $1 \times 3$ and $3 \times 1$ cases the central pipe is held at the fully functional pressure $p_\mathrm{w}$, and equations (1a) and (1b)-(1c) respectively describe the dominance relation between the other two cells. Hence one cell operates under reduced vacuum, next to two adjacent cells under full vacuum. This arrangement assesses to what extent the presence of a third cell affects the results obtained for a pair of cells.

The $2 \times 2$ configuration evaluates the impact due to the presence of both vertical and horizontal neighbouring cells. The symmetry in the horizontal dimension allows for the alteration of the suction in the left pair of wells only without loss of generality (as in the $1 \times 2$ configuration). The dominance fraction $f_p$ is taken positive when the suction in the bottom left well is diminished, i.e. the top well dominates. Similarly, $f_p$ is negative when the suction in the top well is reduced. Thus equations (1b)-(1c) apply to the left pair of wells identically to the $2 \times 1$ configuration. Then the dominance relation of the horizontal pairs of wells is given by (1a), where $f_p$ is taken in its absolute value. Figure 3 shows the expected flux magnitudes. Any upward flux is small and thus significantly affected by gravity, i.e. the two arrangements are not symmetric: the cells contiguous with a dysfunctional cell will always draw the main flux, whilst the third cell will collect the residual ones, however gravity determines the higher one within each pair.

# 4 Results

The FlexPDE solver (PDE Solutions Inc., 2016) was used to obtain a finite element solution with an unstructured triangular, dynamically refined mesh with a prescribed relative error in $p$ (non-dimensionalised by $p_\mathrm{atm}$) of $10^{-7}$. The flux integrals for all configurations were evaluated using the solver's integration functionality.

## 4.1 Horizontal configuration $1 \times 2$

Figure 4 shows the flux across the centre line for a range of suction values $p_\mathrm{w}$. Note the marked linearity throughout the range of $f_p$, but also in $p_\mathrm{w}$, as is evident from comparing the values of $F$ between the three lines for a fixed value of $f_p$. The considered range $\{p_\mathrm{w} \,|\, -3.75 \leqslant p_\mathrm{w} \leqslant -1.25\}$kPa spans the viable working points for landfills of medium size. Moreover, the range of suction values can also be interpreted as well pressure at sections farther upstream from the outlet, so that the presented results are valid for any cross-section in the well. As has been shown in Halvorsen et al. (2018), the flow field with a constant pressure condition on the surface differs significantly from the one with a sealed surface. Figure 13 in appendix B depicts the pressure and horizontal velocity at the centre line as a confirmation. Qualitatively the disparity lies in the normal velocity and is related to the effective permeability (or conversely, resistance) of the boundary. Without a cover the waste matrix evinces a moderate to high permeability and low resistance, whilst the sealed boundary has zero permeability and infinite resistance. Notwithstanding, normalising by the respective value of $F_\mathrm{ref}$ resulted in identical graphs in figure 4.

As the linearity was exhibited for both sealed and permeable surface conditions, it follows that linear behaviour is expected throughout the entire range of feasible permeability of this boundary. Although the gravity force is non-negligible in the balance of vertical momentum throughout the landfill, especially for the no flux surface condition (Halvorsen et al., 2018), the impact of gravity on an integrated quantity such as centre line flux in this configuration was found to be minimal (as expected), as is seen from the relative error in the pressure and velocity profiles along the centre line (figure 14 in appendix B).

Furthermore, the flux graphs for aspect ratios $\ell_x \big/ \ell_y = 2$ and $\ell_x \big/ \ell_y = 3$ normalised by the respective $F_\mathrm{ref}$ are indistinguishable from those corresponding to $\ell_x \big/ \ell_y = 1$. Such invariance of an integrated quantity is stunning, bearing in mind the complexity of the underlying flow field. For instance, the dependence $F_\mathrm{ref}\left(\ell_x \big/ \ell_y\right)$ for either boundary condition is not linear.

## 4.2 Vertical configuration $2 \times 1$

The asymmetry in the vertical configuration is twofold: due to gravity as well as due to boundary conditions when the surface is not sealed. Therefore separate similarity laws must be sought for the two possible surface conditions. Figure

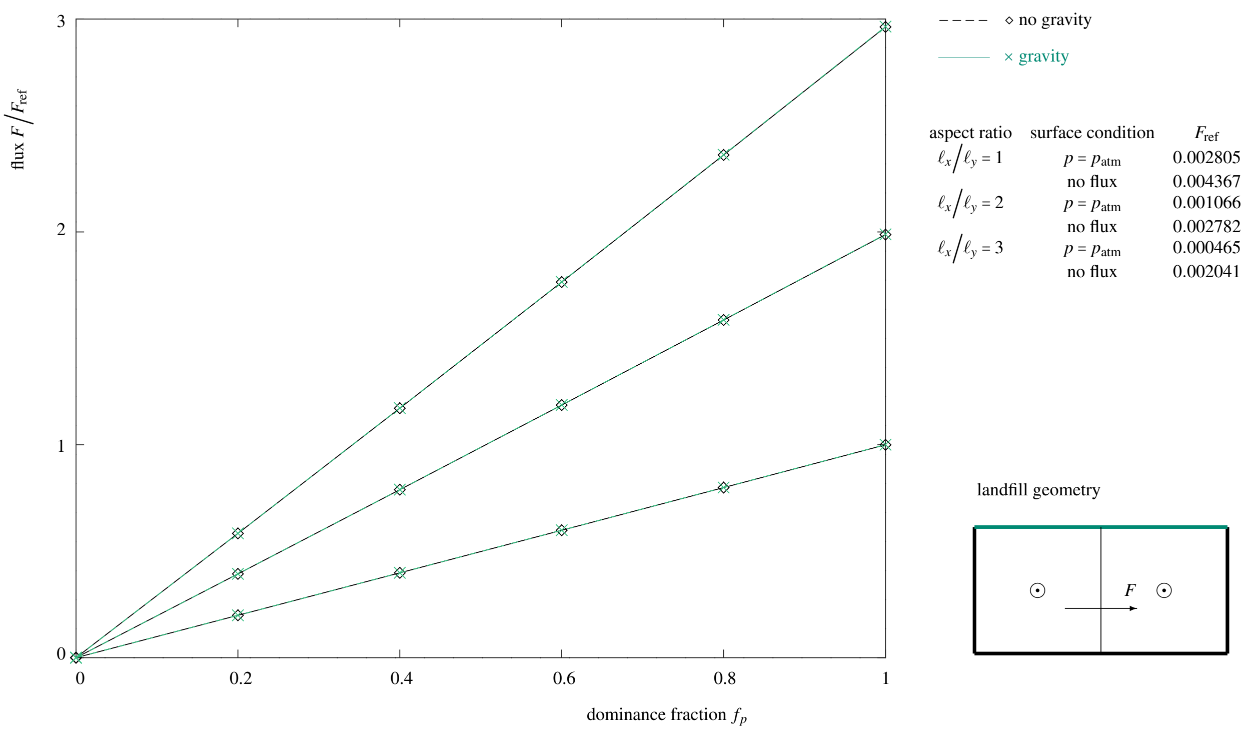


Figure 4: Centre line flux for suction values $p_{\mathrm{w}} = \{-1.25,\ -2.5,\ -3.75\}$kPa (respectively increasing slope) versus pipe dominance fraction $f_p$ in the horizontal $1 \times 2$ configuration (figure 1, reduced schematic shown). $F_{\mathrm{ref}}$ is the value for the case of one well entirely dysfunctional ($f_p = 1$), the other maintaining pressure $p_{\mathrm{w}} = -1.25$kPa, and gravity neglected. Respective $F_{\mathrm{ref}}$ for aspect ratios $1 \leqslant \ell_x/\ell_y \leqslant 3$ and surface boundary conditions are given. All other parameters listed in appendix A

5 shows the centre line flux with an impervious top surface. Whether gravity is accounted for or neglected, the flux function is linear in $f_p$. The normalisation value corresponds to $f_p = 1$, i.e. a dysfunctional bottom well with the top well held at a suction value of $p_{\mathrm{w}} = -1.25$kPa, with gravity taken into account. Linearity in suction strength is evident when comparing the values given by the lines for the three suction values for a fixed $f_p$. The lines obtained with gravity neglected then exhibit a weak non-linearity: the difference between the dimensionless flux values with and without gravity (distance between green/grey and black lines) is almost constant at approximately 0.2, but diminishes slowly toward 0.1 for $f_p$ near 1 and higher suction values. This happens because when the top well is significantly dominant and the imposed suction is sufficiently strong, the effect of gravity is counteracted to some extent. Note that for intermediate values $-1 < f_p < 1$ the relative error incurred due to the omission of gravity can be quite large: the difference of 0.2 is less than 10 per cent at $f_p = -1$ and suction $p_{\mathrm{w}} = -3.75$kPa, but 20 per cent for $p_{\mathrm{w}} = -1.25$kPa, and close to 100 per cent for $f_p = 0.2$. Landfill gas flow is one of scarcely few applications, where gravity cannot be comprehensively disregarded. The quantitative prediction in figure 5 holds for all aspect ratios tested, implying a similarity law analogous to the horizontal configuration. Whilst such a law might have been expected for a setting with a sealed surface and neglected gravity due to symmetry (setting aside the asymmetry due to the well suction), its existence with gravity is remarkable given the large relative error omitting gravity entails.

A configuration with the top surface open to the atmosphere cannot result in a single similarity law, as the dependence of the centre line flux $F$ on suction strength as well as aspect ratio becomes non-linear. Figure 6 depicts $F$ for a landfill of aspect ratio $\ell_x/\ell_y = 1$ and respective graphs for $2 \leqslant \ell_x/\ell_y \leqslant 3$ are given in figures 15–16 in appendix C. The function $F(f_p)$ is linear for the separate regions $f_p \gtrless 0$, but not overall, entailing a curious phenomenon: there exists a critical dominance fraction value $f_{p_{\mathrm{cr}}} > 0$, where lines of the same colour intersect, i.e. $F$ is independent of suction strength. Gravity impacts the flux value at $f_{p_{\mathrm{cr}}}$, but not $f_{p_{\mathrm{cr}}}$ itself. Using $f_{p_{\mathrm{cr}}}$ as a centring point enables a similarity

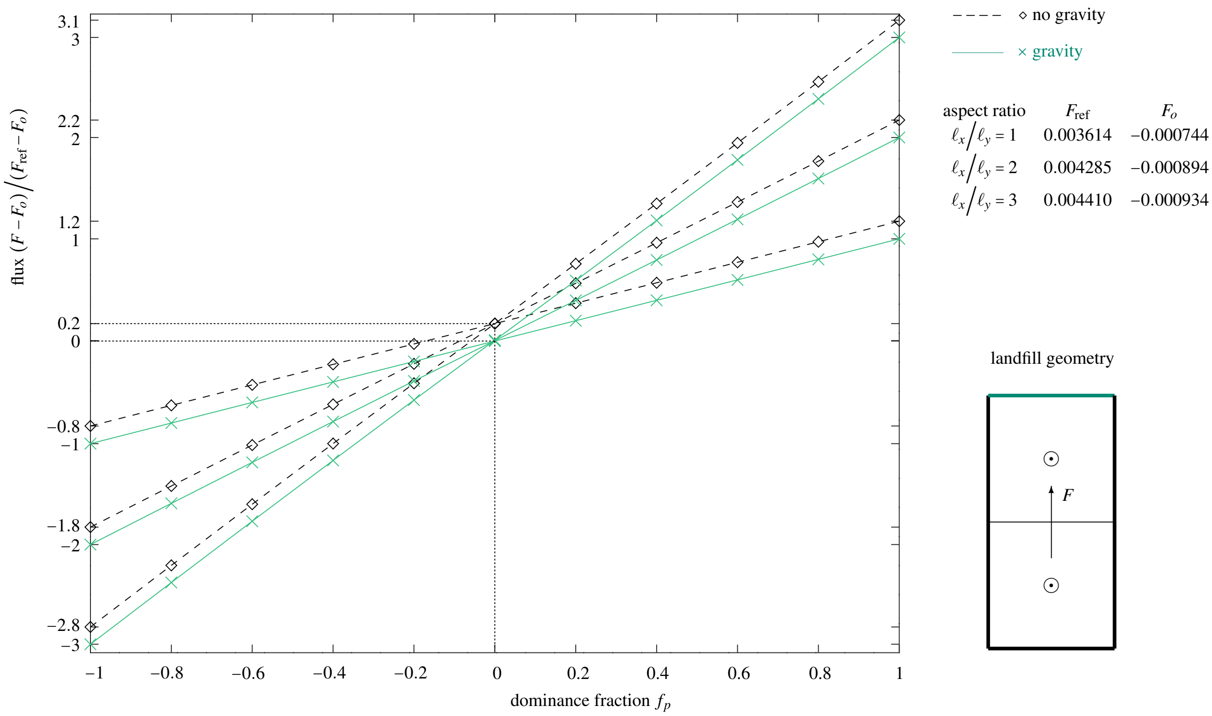


Figure 5: Centre line flux for suction values $p_{\text{w}} = \{-1.25,\ -2.5,\ -3.75\}$kPa (respectively increasing slope) versus pipe dominance fraction $f_p$ in the vertical $2 \times 1$ configuration (figure 2, reduced schematic shown) with a sealed surface. $F_{\text{ref}}$ is the value for the case of bottom well entirely dysfunctional ($f_p = 1$), top well maintaining pressure $p_{\text{w}} = -1.25$kPa, and gravity accounted for. $F_o$ is the value for equally dominant wells ($f_p = 0$). Respective $F_{\text{ref}}$ and $F_o$ values for aspect ratios $1 \leqslant \ell_x / \ell_y \leqslant 3$ are given. All other parameters listed in appendix A

law with respect to suction strength for $f_p > 0$: this is evident from the linear growth of the normalised flux value between the three lines for a fixed value of $f_p$, both with and without gravity. $f_{p_{\text{cr}}}$ grows with landfill aspect ratio, but at the higher aspect ratios this growth slows down as the well's radius of influence is reached and more landfill gas escapes collection.

At first glance attaining a similarity law for the range $f_p < 0$ appears impossible, however the common feature unifying all aforementioned cases, where such a law ensued, was the existence of a single intersection point for the lines representing different suction strength values. When the flux $F_o$ at this intersection point was used to centre the lines and for instance the flux $F_{\text{ref}}$ at $|f_p| = 1$ to scale them, all lines in figures 4 and 5 collapsed onto a single line connecting the points $(-1, -1)$ and $(1, 1)$, i.e. basically

$$(F - F_o) \Big/ (F_{\text{ref}} - F_o) = f_p \tag{4}$$

for any suction strength, aspect ratio and boundary condition. When this procedure is performed separately for $f_p \gtrless 0$ for data from figures 6, 15 and 16, figure 7 ensues, proving that the dependence on suction strength, boundary condition and inclusion / omission of gravity as well as $f_{p_{\text{cr}}}$ disappears. The only remaining dependence is on the aspect ratio, as is seen from the listed line equations. Note that the coefficients of the equations are virtually linear in aspect ratio and thus an additional tier of normalisation would result in a single formula (still split for $f_p \gtrless 0$) similar to equation (4). In the field the completion of this procedure is somewhat involved, as data from the same landfill will be required over several stages of expansion. Construction of either of the two lines for $f_p \gtrless 0$ and usage for prediction of the mass of gas collected for a landfill of a given aspect ratio requires the preliminary identification of the intersection point, whereupon it is identical to the horizontal $1 \times 2$ configuration.

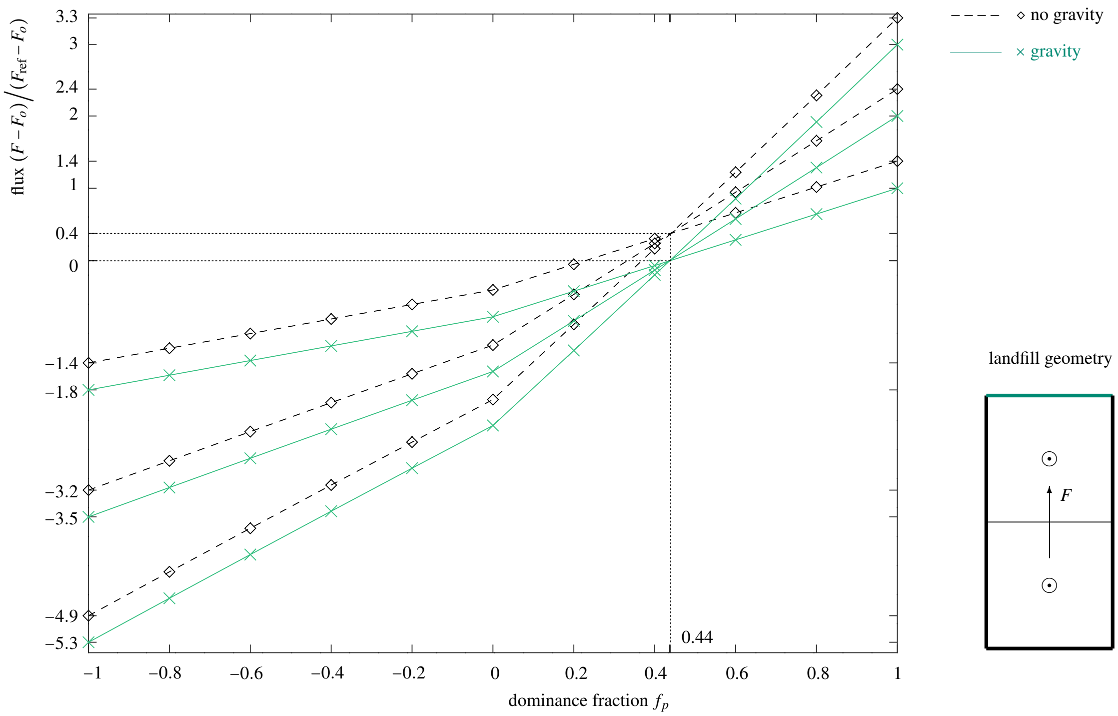


Figure 6: Centre line flux for suction values $p_\text{w} = \{-1.25,\ -2.5,\ -3.75\}$kPa (respectively increasing slope) versus pipe dominance fraction $f_p$ in the vertical $2 \times 1$ configuration (figure 2, reduced schematic shown) with $p = p_\text{atm}$ on the surface. $F_\text{ref} = 0.002709$kg/(m s) is the value for the case of bottom well entirely dysfunctional ($f_p = 1$), top well maintaining pressure $p_\text{w} = -1.25$kPa, and gravity accounted for. $F_o = 0$ is the respective suction independent value ($f_{p_\text{cr}} = 0.44$). Aspect ratio $\ell_x/\ell_y = 1$. All other parameters listed in appendix A

The discontinuity at $f_p = 0$ is a direct result of the slope break in all lines in figures 6, 15 and 16 and an artefact of the necessity to use separate intersection points for $f_p \gtrless 0$. Whilst for $f_p > 0$ the intersection point has the physical meaning of $f_{p_\text{cr}}$ and falls within the relevant range $0 < f_p < 1$, the concomitant point for $f_p < 0$ lies outside the range $-1 < f_p < 0$ and possesses no physical relevance beyond serving as a mathematical tool to obtain the similarity law.

## 4.3 Practical application

Given that the flow equations (2) are non-linear and not soluble analytically in domains that realistically represent the landfill geometry, the extensive similarity is an interesting and unexpected finding. In conjunction with the exhibited linear behaviour of the normal flux between adjacent cells it is conducive of building empirical models, when practitioners have no access to advanced numerical computation. Since the flux across the centre line equals the difference in the mass collected by the two wells, the foregoing qualitative results enable immediate quantitative predictions in the field as follows.

The vertical $2 \times 1$ configuration with a sealed surface and the horizontal $1 \times 2$ configuration with any type of condition on the surface are only weakly asymmetric and possess full similarity throughout the parameter space. In particular the critical value of the dominance fraction is $f_{p_\text{cr}} = 0$, i.e. wells operating under equal suction. It is sufficient to note the value $F_o$ at this setting as well as the value $F_\text{ref}$ at any non-zero value $f_p$, in order to construct one straight line $F(f_p)$. Implementing the similarity laws, this function can be used for prediction of the flux (difference in production between the two wells) under any suction value or suction asymmetry condition. Pertinent situations, where such predictions are helpful, are failing vacuum blowers and replacement thereof with stronger or weaker models, as well as possible damage to the bottom pipe in the $2 \times 1$ configuration. Pre-constructing the function whilst the landfill is

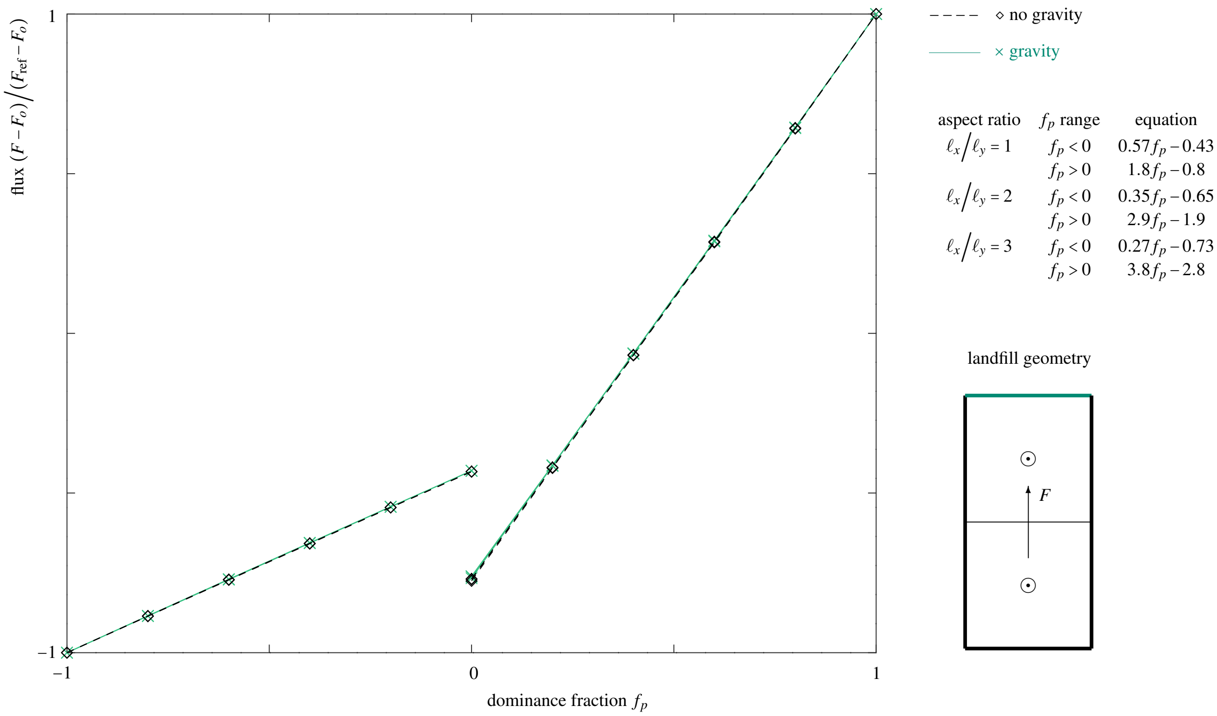


Figure 7: Self-similarity of all data in figures 6, 15 and 16. The marked values on the ordinate are correct by definition, but the lines are not to scale; for exact proportions see line equations for different aspect ratios given to precision of two significant figures

fully functional (or projecting expected values in the design stage) permits to infer to what extent the remaining pipe would be able to compensate for its failing neighbour. The inverse inference is also possible: given an asymmetric suction application and a desired production, it is possible to compute the required blower strength. Furthermore, if the cell is expanded to a greater aspect ratio or an additional well is installed, diminishing the aspect ratio, designating a reference point on a formerly obtained line and correcting by the new flux at the same operational point will accord all required predictions for the new configuration. The line coefficients can be easily updated during the landfill's lifetime.

The vertical $2 \times 1$ configuration with a partly permeable surface is a strongly asymmetric setting. Here the above analysis is somewhat more involved. Whilst the qualitative behaviour remains linear, $f_{p_{\text{cr}}} \neq 0$ and it is necessary to split the function for $f_p \gtrless 0$. The vacuum blower should be tuned between two or three values and production of the two wells for the values $f_p = -1, 0, 1$ recorded. Constructing the respective lines and and calculating their intersection point separately for $f_p \gtrless 0$ yields $f_{p_{\text{cr}}}$. The flux at that point is $F_o$. $F_{\text{ref}}$ is the value at some $f_p > 0$. Then formula (4) predicts $F$. The effect of gravity is more pronounced when $f_p < 0$, i.e. the bottom well suction is weaker and fluid travels against the gravity field to the top well. For this reason the linearity in nominal suction strength is slightly impaired for $f_p < 0$ (an error of 1–3 per cent with the bottom well completely dysfunctional at $f_p = -1$), as is seen by comparing the distance between the green/grey lines for a fixed $f_p$ in figures 6, 15 and 16. This small deviation is not expected to compromise practical use.

## 4.4 Localisation in multi-cell configurations

A realistic landfill rarely comprises only one or two cells. It is hereby conjectured that the above analysis can be applied to configurations of multiple cells upon division into suitable units of two cells. This section's purport is to supply numerical evidence justifying such an approach.

Beginning with the $1 \times 3$ horizontal configuration, the following comparison was performed. The conditions in the

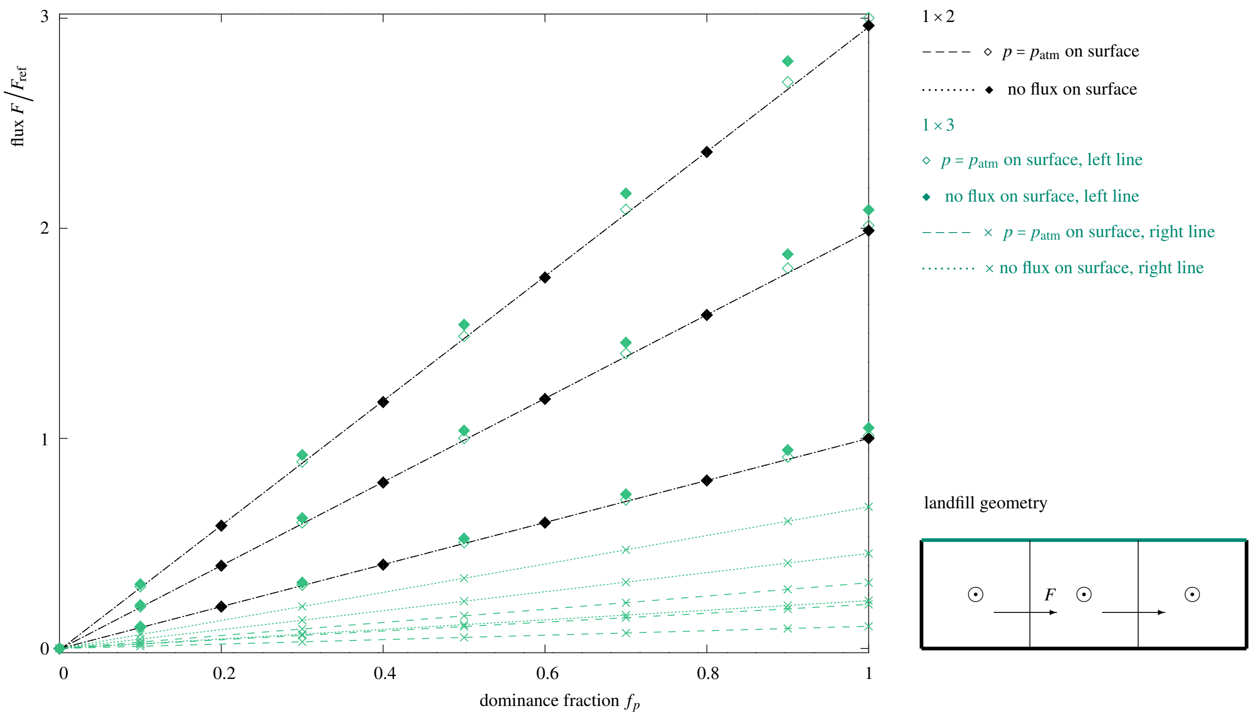


Figure 8: Line flux for suction values $p_{\mathrm{w}} = \{-1.25,\ -2.5,\ -3.75\}$kPa (respectively increasing slope) versus pipe dominance fraction $f_p$ in the horizontal $1 \times 3$ configuration (reduced schematic shown) with no gravity. $F_{\mathrm{ref}}$ is the value for the case of the left well entirely dysfunctional ($f_p = 1$), the other two maintaining pressure $p_{\mathrm{w}} = -1.25$kPa. Aspect ratio $\ell_x / \ell_y = 1$. $F_{\mathrm{ref}}$ values are given in figure 4. All other parameters listed in appendix A

central and right cells were kept fixed. The suction strength of the left cell was diminished according to equation (1a). The flux across the left wall of the central cell was juxtaposed with the respective flux in the $1 \times 2$ configuration in figure 8. Using the least squares technique, a straight line was fitted through the points of the $1 \times 2$ configuration, whereupon the points of the $1 \times 3$ configuration were added to the graph. The visual agreement implies that essentially the flux between the left and central cells depends on the relative dominance between those two cells and is independent of the state of the right cell. The relative error was up to 1 per cent for the boundary condition of constant pressure on the surface and 5 per cent for a sealed surface. The larger error in the latter case was incurred due to the fact that more gas was collected, when the sealed top impeded gas escape to the atmosphere. The respective least squares fit errors were up to 0.1 per cent and 0.5 per cent. For aspect ratios $2 \leqslant \ell_x / \ell_y \leqslant 3$ the graphs were qualitatively similar and thus are not shown. Moreover, the foregoing fit errors between the $1 \times 3$ and $1 \times 2$ configurations diminished to the least squares fit errors of the latter, substantiating the finding that essentially the state of the adjacent cell determines the flux. The lesser suction at the left cell entailed a small flux (an order of magnitude less) across the wall between the central and right cells, albeit their suction strength was equal. This residual flux is amenable to the self-similarity laws discussed heretofore, however no coherent quantitative relation was found to connect it with the main flux.

The analysis of the vertical $3 \times 1$ configuration is a similar extension of the $2 \times 1$ counterpart. The central cell suction strength was held fixed. The relative dominance fraction between the bottom and top cells was determined by equations (1b) – (1c). All simulations included gravity, as the effect thereof had already been proved non-negligible. Figure 9 shows the dimensional flux across the contiguity lines between the cells superimposed upon the $2 \times 1$ centre line flux. As with the $1 \times 3$ array, there is a strong flux (referred to as main) between the central cell and the one with the diminished suction, and an order of magnitude weaker (residual) flux between the central cell and the other dominant cell. The main flux is well correlated with the central line flux of the $2 \times 1$ configuration, however the agreement deteriorates with aspect ratio: the maximal error (occurring for a dominant bottom cell, where the asymmetry due to

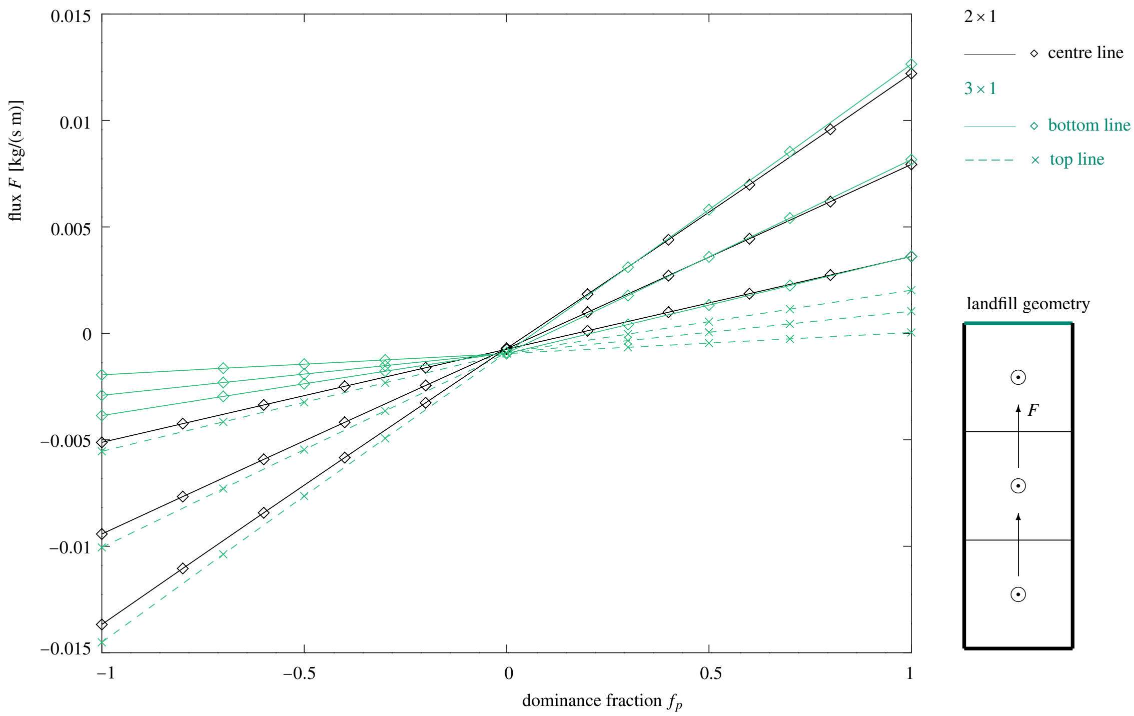


Figure 9: Line flux (dimensional) for suction values $p_w = \{-1.25,\ -2.5,\ -3.75\}$kPa (respectively increasing slope) versus pipe dominance fraction $f_p$ in the vertical $3 \times 1$ configuration (reduced schematic shown) with a sealed surface, gravity accounted for, aspect ratio $\ell_x \big/ \ell_y = 1$ and central well maintaining pressure $p_w = -1.25$kPa. All other parameters listed in appendix A

gravity is further enhanced by the differences in suction strength) grows from about 5 per cent for $\ell_x \big/ \ell_y = 1$ to 20 per cent at $\ell_x \big/ \ell_y = 3$. Notably both the main and residual fluxes are linear throughout the range $-1 \leqslant f_p \leqslant 1$, i.e. there is no break in the slope at $f_p = 0$ as the dominance is switched from the bottom cell to the top, as is the case with a permeable cover, cf. figures 6, 15 and 16. Bearing in mind that the gravity effect is not symmetric, this is not a trivial conclusion. Hence it is possible to seek self-similarity as for the $2 \times 1$ configuration, and the two are compared in figure 10 for all tested aspect ratios.

From the results of the $2 \times 1$ configuration, when the surface is not sealed, no self-similarity is expected as the three independent sources of asymmetry (boundary condition, suction strength and gravity) render the flow field highly asymmetric. Both the main and residual fluxes exhibited qualitative behaviour as in the $2 \times 1$ configuration, i.e. linearity for $f_p \gtrless 0$ and an intersection point $f_{p_{\mathrm{cr}}}$, where the flux is independent of the dominance fraction (consult figures 6, 15 and 16), and hence were amenable to representation as in figure 7 (quantitative results not shown).

The $2 \times 2$ configuration tested the robustness of the foregoing findings to the proximity of horizontal as well as vertical neighbour cells. Consider first a landfill with a sealed surface. Figure 11 depicts a dimensional example of the flux across the contiguity walls between the cells. The total flux across the vertical centre line was equal to the concomitant of the $1 \times 2$ configuration (dashed and dotted green/grey lines, identical for $f_p \lesseqgtr 0$). The vertical flux requires a more cautious approach. For instance, when the suction is diminished in the bottom left well, some of the gas generated in that cell travels into the other three cells. The highest amount is collected by the bottom right well, whilst the top left well collects a comparable, but slightly reduced amount due to gravity. Most of the mass moving laterally between the bottom pair of cells is absorbed by the right well. Notwithstanding, a residual flux does continue vertically into the top right cell. Hence in comparison of the flux across the horizontal centre line of $2 \times 2$ and $2 \times 1$ arrays, only the flux across the left half of the line should be taken in the former case, so as not to include

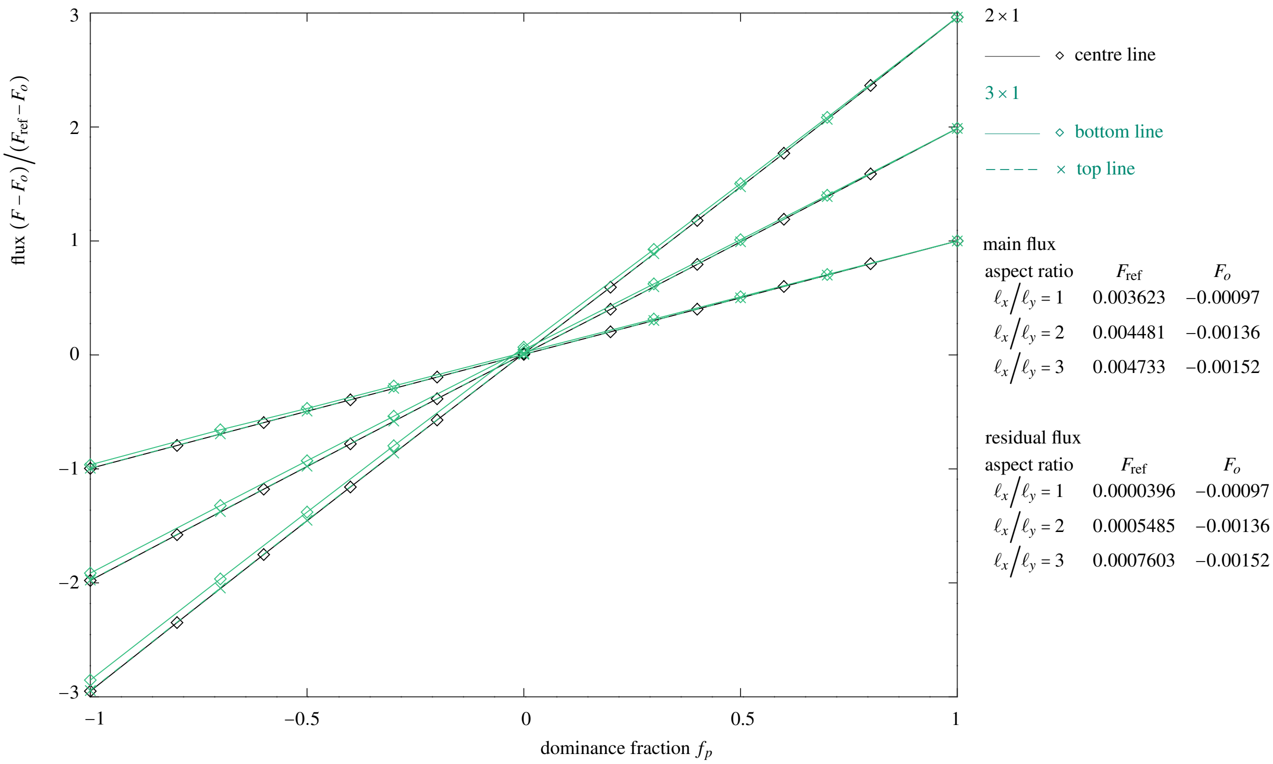


Figure 10: Line flux (non-dimensional) for suction values $p_{\text{w}} = \{-1.25,\ -2.5,\ -3.75\}$kPa (respectively increasing slope) versus pipe dominance fraction $f_p$ in the vertical $3 \times 1$ configuration (reduced schematic shown in figure 9) with a sealed surface, gravity accounted for and central well maintaining pressure $p_{\text{w}} = -1.25$kPa. $F_{\text{ref}}$ is the value for the case of bottom well entirely dysfunctional ($f_p = 1$), top well maintaining pressure $p_{\text{w}} = -1.25$kPa. $F_o$ is the value for equally dominant wells ($f_p = 0$). Respective $F_{\text{ref}}$ and $F_o$ values for aspect ratios $1 \leqslant \ell_x\big/\ell_y \leqslant 3$ are given. All other parameters listed in appendix A

any superfluous mass counted both as a horizontal flux between the left and right bottom cells, and as a vertical flux between the bottom and top right cells. Overall the flux between the left pair of cells is expected to be slightly less than that in the $2 \times 1$ configuration due to the possibility of lateral escape to the right half of the landfill. The quantitative agreement between the vertical flux in the left half of the landfill and the $2 \times 1$ counterpart improves with aspect ratio, as said lateral escape is minimised (black dashed and dotted lines). All of the above fluxes obey similarity laws and exhibit linearity in suction strength, as confirmed in figure 12.

As anticipated, with a partly permeable surface no insightful quantitative behaviour could be gleaned, albeit qualitatively the same properties were recovered as for $1 \times 3$ and $3 \times 1$ configurations (linearity and $f_{p_{\text{cr}}}$). Hence all fluxes can be represented as in figure 7.

## 5 Conclusion

Gas collection wells in medium and large landfills induce a flow field that to this day has not been fully fathomed. The gas is generated in the waste matrix and flows through a highly heterogeneous porous medium. The fluid compressibility and compound resistance of the anisotropic medium and boundaries renders the design and controllability of this system challenging. Relatively fast temporal evolution further exacerbates the efforts to create models that would provide accurate predictions pertinent to a specific site. The analysis presented herein uses an approach unconventional in the solid waste management field: the partial differential equations governing the flow of ideal gas through a

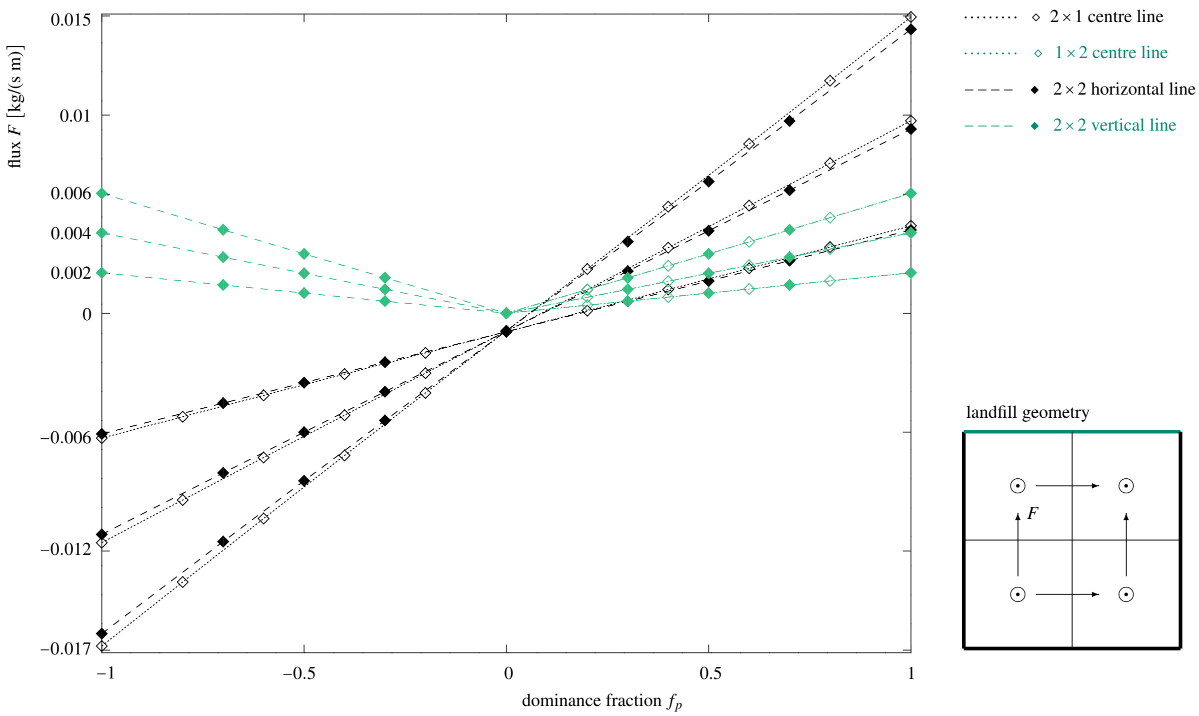


Figure 11: Line flux (dimensional) for suction values $p_w = \{-1.25,\ -2.5,\ -3.75\}$kPa (respectively increasing slope) versus pipe dominance fraction $f_p$ in the $2 \times 2$ configuration (figure 3, reduced schematic shown) with a sealed surface, gravity accounted for, aspect ratio $\ell_x \big/ \ell_y = 3$ and right wells maintaining pressure $p_w = -1.25$kPa. All other parameters listed in appendix A

porous medium were solved for a wide range of operational conditions, whereupon normal flux between cells drained by distinct horizontal wells was shown to obey similarity laws. This simple qualitative behaviour can now be used in quantitative custom modelling by fitting the flow rate data routinely recorded for each well, and with no need to repeat the exhaustive numerical computations. Circumstances where self-similarity deteriorates are discussed hereunder.

One particular aspect of interest is the interference between adjacent wells. The need to predict mutual response of wells draining several proximate cells might arise many times during the lifetime of a landfill. Some examples are (a) an expansion, either lateral or vertical, resulting in new cells interacting with existing ones; (b) waste settlement and consequent diminution of gas generation rate, whereupon operators would consider installing additional wells as part of the refilling stage; (c) ineffectual function of existing wells due to clogging or inundation by leachate or risen water table, when it might stand to reason to instal new wells at a lesser depth, whilst leaving the older wells functioning at their partial capacity. In the last example liquid levels are known to fluctuate, so prediction of the well response from full function ($f_p = 0$) to complete failure ($|f_p| = 1$) is of use. In light of the above the main focus was on realistic geometry in conjunction with asymmetric operational conditions. Asymmetry due to a partly permeable surface, gravity, unequal suction strength at multiple collection wells and combinations thereof was considered. It was shown that integrated quantities such as normal flux across a contiguity plane between two adjacent cells might exhibit a markedly simple behaviour over a stunningly wide range of parameters.

What makes the normal flux a unique quantity in landfill gas flow field modelling is its immediate accessibility in the field. In contrast to many modelling parameters associated with this flow field – fluid pressure and velocity, medium permeability and numerous others, the normal flux is just about the only parameter that can be obtained with little effort and high certainty: it is simply the difference in the mass of gas collected by adjacent wells as measured at the wellheads. Owing to the simplicity of its acquisition, this quantity can be tracked over time and all concomitant models adjusted accordingly with relative ease. The landfill system is complex and fast changing. The

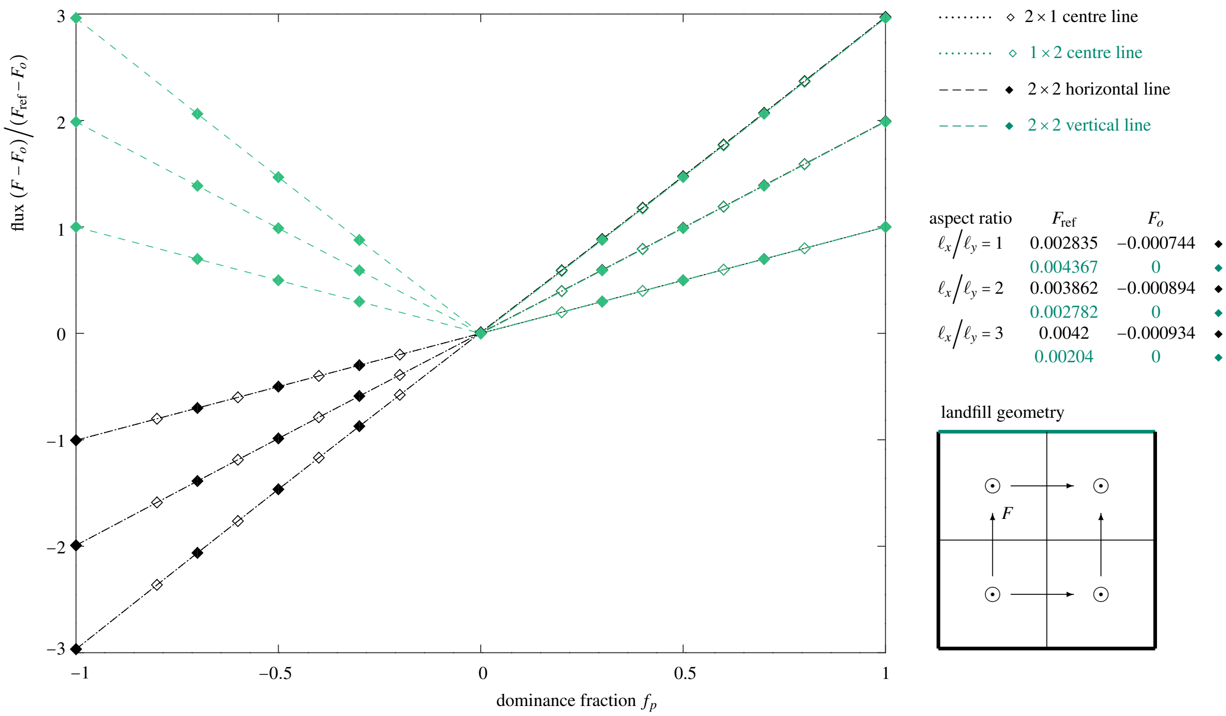


Figure 12: Line flux (non-dimensional) for suction values $p_{\text{w}} = \{-1.25,\ -2.5,\ -3.75\}$kPa (respectively increasing slope) versus pipe dominance fraction $f_p$ in the $2 \times 2$ configuration (figure 3, reduced schematic shown) with a sealed surface, gravity accounted for and right wells maintaining pressure $p_{\text{w}} = -1.25$kPa. Respective $F_{\text{ref}}$ and $F_o$ values for aspect ratios $1 \leqslant \ell_x\big/\ell_y \leqslant 3$ are listed. All other parameters listed in appendix A

anisotropy of the waste content as well as degradation rate is the salient impediment to efficient modelling of landfill gas flow: the former renders evaluating any local parameter an impracticable endeavour, whilst the latter detracts from the worthwhileness of estimating effective (spatially averaged) quantities. Thus models that are accessible to field operators, simple to implement and adjust over the landfill's lifetime, are an important step.

The main factor affecting the behaviour of the flux between cells is the number of asymmetry sources. With small to medium asymmetry the flux manifests bi-linearity with respect to the dominance fraction (relative suction strength) as well as absolute suction strength, and the dependence on both is self-similar in aspect ratio. For example, in the $1 \times 2$ configuration the main source of asymmetry would be a partly permeable cover, whilst gravity would have a much weaker effect. With a sealed cover, the only source of asymmetry is gravity, and both cases would fall into the small to medium asymmetry category. When more cells are positioned in a row, as in the $1 \times 3$ configuration, the geometric asymmetry of suction points is added, entailing a small deviation from the perfect two-cell self-similarity. In practice it would be reasonable to focus the modelling on any two adjacent cells out of a row, providing that the weaker wells are separated by at least two fully functional ones.

In vertically stacked cells the gravity becomes an important physical factor, so that with an impervious cover the asymmetry is still medium, however with a partly permeable surface the asymmetry is high enough for the overall linearity in the dominance fraction $f_p$ to break down. Nonetheless the linearity is retained separately for the ranges $f_p \gtrless 0$, i.e. as long as one well is designated as the reference well and its suction strength is held fixed, the flux is linear with respect to the reduced vacuum in the adjacent well. There exists a critical value $f_{p_{\text{cr}}}$, where the flux is independent of suction strength. The linearity in suction strength is impaired slightly, however the practical use of self-similarity should not be impeded in any way. The analysis is valid for configurations of three cells and more with the same stipulation as for horizontal arrays. The $2 \times 2$ configuration was used to confirm the above conclusions for arrays extending in both directions.

The two surface boundary conditions – sealed and partly permeable – delimit the moderate to extremely low interval of feasible operating permeabilities. The existence of exact similarity laws for an impervious cover and a minor deterioration of bi-linearity as the cover resistance is diminished, allow to conjecture that using these models under most operating conditions would entail only a small error. The landfill engineers would be able to quantify the error by constructing additional lines $F(f_p)$ as required.

The analysis is valid for any cell aspect ratio as long as adjacent cells are within each other's radii of influence. Ultimately for any given suction value there exists a cell so oblate $\left(\ell_x \big/ \ell_y \gg 1\right)$ that gas generated near its borders is not collected. In this working regime the relationship between two neighbour cells that was studied here, disintegrates. In the field this state is evidenced if diminution of suction strength in one of the wells results in no impact on the flow of the other. Some means of control of the radius of influence are outlet vacuum, perforation density and boundary resistance (Nec and Huculak, 2019).

In summary, the flow field of landfill gas in configurations with multiple suction points was studied for effects of asymmetry. In adjacent horizontal cells the flux across the centre line induced by unequal suction was found to be a linear function of the difference in suction strength as well as of the suction strength itself. The non-dimensionalised flux is invariant with respect to the cell aspect ratio and the surface boundary condition. This self-similarity in conjunction with bi-linearity enables practicable predictions in the field to aid in the operation and modification of one or multiple cells. The linearity and self-similarity hold for a wide range of operational parameters corresponding to a medium sized landfill, but deviations therefrom are observed under highly asymmetric conditions, such as in vertically stacked cells with a partly permeable surface, where gravity becomes an important source of asymmetry. Based on the analysis an adjustable modelling technique is suggested. The presented models are simple to construct, customise, implement and update over the lifetime of a given landfill.

## Acknowledgement

Field data furnished by GNH Consulting Ltd., Delta, British Columbia, Canada, are gratefully acknowledged.

## References


Abichou T, Mahieu K, Yuan L, Chanton J, Hater G (2009) Effects of compost biocovers on gas flow and methane oxidation in a landfill cover. Waste Management 29:1595–1601

Barlaz MA, Chanton JP, Green RB (2009) Controls on landfill gas collection efficiency: instantaneous and lifetime performance. J Air and Waste Management Association 59(12):1399–1404

Barnes KK, Christenson SC, Kolpin DW, Focazio MJ, Furlong ET, Zaugg SD, Meyer MT, Barber LB (2004) Pharmaceuticals and other organic waste water contaminants within a leachate plume downgradient of a municipal landfill. Ground Water Monitoring and Remediation 24(2):119–126

Christensen TH, Kjeldsen P, Bjerg PL, Jensen DL, Christensen JB, Baun A, Albrechtsen HJ, Heron G (2001) Biogeochemistry of landfill leachate plumes. Applied Geochemistry 16(7–8):659–718

Davidson TA (1993) A simple and accurate method for calculating viscosity of gaseous mixtures. Report of investigations, US Department of the Interior, Bureau of Mines.

Durmusoglu E, Corapcioglu MY, Tuncay K (2005) Landfill settlement with decomposition and gas generation. J Environ Eng 131(9):1311

Feng SJ, Zheng QT, Xie HJ (2015) A model for gas pressure in layered landfils with horizontal gas collection systems. Comput Geotech 68:117–127

Feng SJ, Zheng QT, Xie HJ (2017) A gas flow model for layered landfills with vertical extraction wells. Waste Management 66:101–113

Findikakis AN, Leckie JO (1979) Numerical simulation of gas flow in sanitary landfills. J Environ Eng Div 105(5):927–945

Fulks WB, Guenther RB, Roetman EL (1971) Equations of motion and continuity for fluid flow in a porous medium. Acta Mechanica 12:121–129

Gebert J, Groengroeft A (2006) Passive landfill gas emission - influence of atmospheric pressure and implications for the operation of methane-oxidising biofilters. Waste Management 26(3):245–251

Gioannis GD, Muntoni A, Cappai G, Milia S (2009) Landfill gas generation after mechanical biological treatment of municipal solid waste. estimation of gas generation rate constants. Waste Management 29(3):1026–1034

Halvorsen D, Nec Y, Huculak G (2018) Horizontal landfill gas wells: geometry, physics of flow and connection with the atmosphere. Physics and Chemistry of the Earth 113:50–62

Lu AH, Kunz CO (1981) Gas-flow model to determine methane production at sanitary landfills. Environ Sci Technol 15(4):436–440

Lyngkilde J, Christensen TH (1992) Redox zones of a landfill leachate pollution plume (Vejen, Denmark). J Contaminant Hydrology 10(4):273–289

Nec Y, Huculak G (2019) Landfill gas flow: collection by horizontal wells. Transport in Porous Media 130(3):769–797

Panda MN, Lake LW (1994) Estimation of single-phase permeability from parameters of particle-size distribution. American Association of Petroleum Geologists Bulletin 78(7):1028–1039

PDE Solutions Inc. (2016) Flexpde 7. *http://www.pdesolutions.com*

Spokas K, Bogner J, Chanton JP, Morcet M, Aran C, Graff C, Golvan YML, Hebe I (2006) Methane mass balance at three landfill sites: what is the efficiency of capture by gas collection systems? Waste Management 26(5):516–525

Whitaker S (1986) Flow in porous media I: a theoretical derivation of Darcy's law. Transport in Porous Media 1:3–25

Wise WR, Townsend TG (2011) One-dimensional gas flow models for municipal solid waste landfills: cylindrical and spherical symmetries. J Environ Eng 137(6):514–516

Wiszniowski J, Robert D, Surmacz-Gorska J, Miksch K, Weber JV (2006) Landfill leachate treatment methods: a review. Env Chem Lett 4(1):51–61

Young A (1989) Mathematical modeling of landfill gas extraction. J Environ Eng 115(6):1073–1087

## Appendix A. Base parameters

Table 1 lists the nominal set of parameters used in computations throughout unless noted specifically in pertinent figure captions. Negative pressure values are relative to the atmosphere.

| parameter | value |
|---|---|
| pipe radius | 0.0762 m (3 in) |
| tortuosity | 100 |
| temperature | 15$^o$C |
| suction vacuum | −1.25 kPa |
| surface pressure | −0.125 kPa |
| generation rate | 0.004 kg/(m$^3$hr) |
| $CH_4$ molar fraction | 0.5 |
| $O_2$ molar fraction | 0.01 |
| $CO_2$ molar fraction | 0.4 |
| gravel thickness | 1 m |
| waste depth | 8 m |
| gravel porosity | 0.6 |
| waste porosity | 0.4 |
| gravel fragment size | 0.025 m |
| waste fragment size | 0.05 m |

Table 1: Parameters of a single landfill cell common to all examples solved numerically

## Appendix B. Horizontal configuration 1 × 2: supplemental figures

Figure 13 exemplifies the disparity of the pressure and horizontal velocity profiles along the centre line in the horizontal $1 \times 2$ configuration. Figure 14 shows the typical error magnitude for both variables when neglecting the gravitational force in the balance of vertical momentum for the boundary conditions of atmospheric pressure and sealed surface.

## Appendix C. Vertical configuration 2 × 1: supplemental figures

Figures 15 and 16 give the centre line flux with atmospheric pressure on the top surface for aspect ratios $\ell_x / \ell_y = 2$ and $\ell_x / \ell_y = 3$ respectively. The construction of these similarity lines is explained in detail for $\ell_x / \ell_y = 1$ in §4.2.

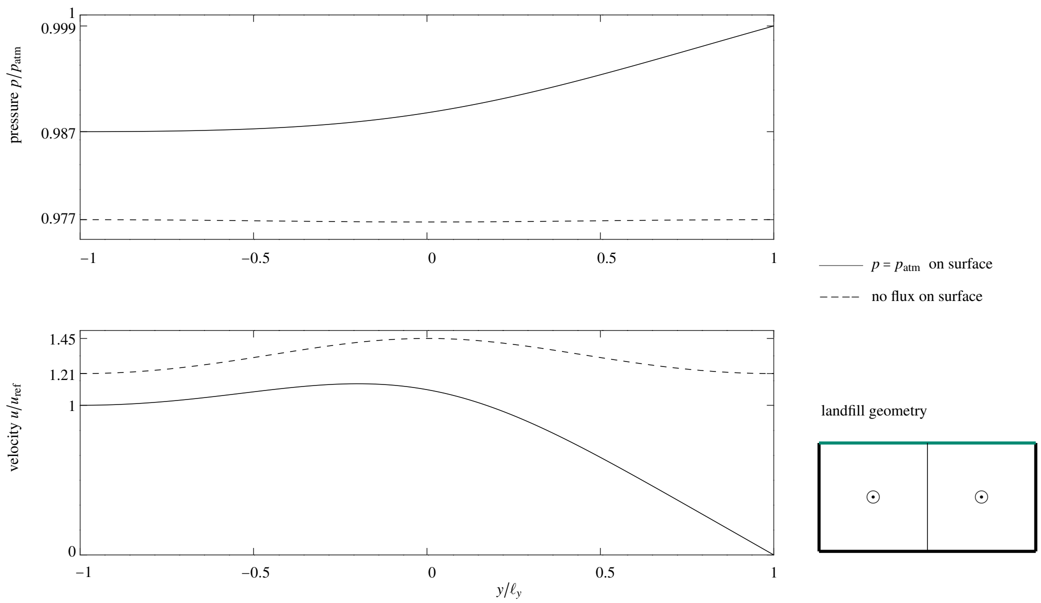


Figure 13: Pressure (upper panel) and horizontal velocity (lower panel) profile along the centre line for suction value $p_{\text{w}} = -3.75\text{kPa}$ in the horizontal $1 \times 2$ configuration (figure 1, reduced schematic shown) with $f_p = 0.5$, aspect ratio $\ell_x \big/ \ell_y = 1$ and gravity neglected. $u_{\text{ref}}$ is the value at landfill bottom for the boundary condition $p = p_{\text{atm}}$ on the surface. All other parameters listed in appendix A

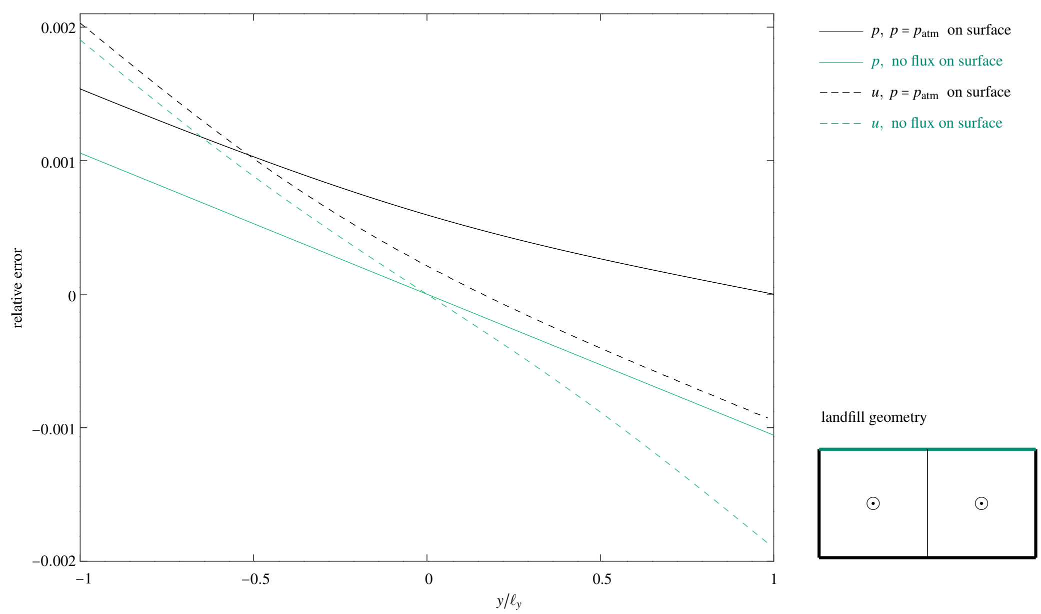


Figure 14: Neglecting gravity: error in pressure $p$ and horizontal velocity $u$ along the centre line for suction value $p_{\text{w}} = -3.75\text{kPa}$ in the horizontal $1 \times 2$ configuration (figure 1, reduced schematic shown) with $f_p = 0.5$ and aspect ratio $\ell_x \big/ \ell_y = 1$. All other parameters listed in appendix A

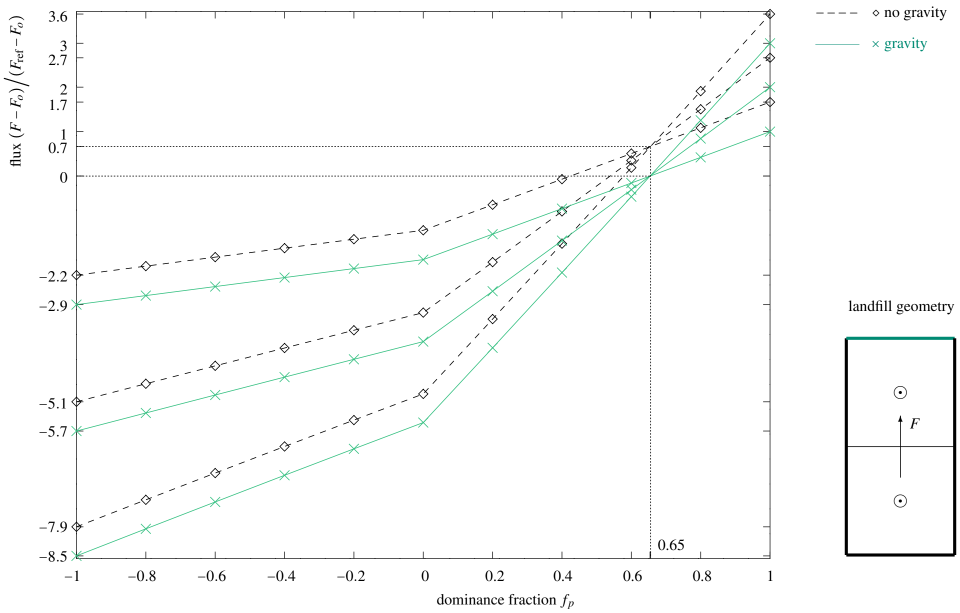


Figure 15: Centre line flux for suction values $p_w = \{-1.25, -2.5, -3.75\}$kPa (respectively increasing slope) versus pipe dominance fraction $f_p$ in the vertical $2 \times 1$ configuration (figure 2, reduced schematic shown) with $p = p_{atm}$ on the surface. $F_{ref} = 0.004894$kg/(m s) is the value for the case of bottom well entirely dysfunctional ($f_p = 1$), top well maintaining pressure $p_w = -1.25$kPa, and gravity accounted for. $F_o = 0.002591$kg/(m s) is the respective suction independent value ($f_{p_{cr}} = 0.65$). Aspect ratio $\ell_x / \ell_y = 2$. All other parameters listed in appendix A

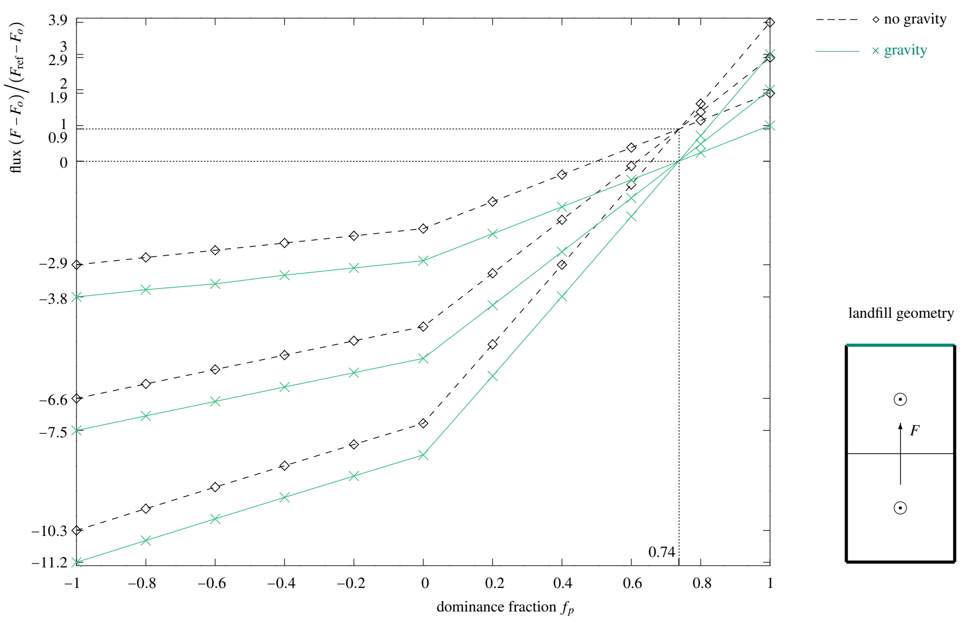


Figure 16: Centre line flux for suction values $p_w = \{-1.25, -2.5, -3.75\}$kPa (respectively increasing slope) versus pipe dominance fraction $f_p$ in the vertical $2 \times 1$ configuration (figure 2, reduced schematic shown) with $p = p_{atm}$ on the surface. $F_{ref} = 0.00872$kg/(m s) is the value for the case of bottom well entirely dysfunctional ($f_p = 1$), top well maintaining pressure $p_w = -1.25$kPa, and gravity accounted for. $F_o = 0.00674$kg/(m s) is the respective suction independent value ($f_{p_{cr}} = 0.74$). Aspect ratio $\ell_x / \ell_y = 3$. All other parameters listed in appendix A